RESEARCH PAPER

Fast stomatal kinetics in sorghum enable tight coordination with photosynthetic responses to dynamic light intensity and safeguard high water use efficiency

Martin W. Battle[iD], **Silvere Vialet-Chabrand**[†,iD], **Piotr Kasznicki**[iD], **Andrew J. Simkin**[iD], **and Tracy Lawson**[*,iD]

School of Life Sciences, University of Essex, Wivenhoe Park, Colchester CO4 3SQ, UK
[†] Present address: Horticulture and Product Physiology; WUR; Droevendaalsesteeg 1, 6708PB, Wageningen, The Netherlands.

[*] Correspondence: tlawson@essex.ac.uk

Abstract

In this study, we assessed 43 accessions of sorghum from 16 countries across three continents. Our objective was to identify stomatal and photosynthetic traits that could be exploited in breeding programmes to increase photosynthesis without increasing water use under dynamic light environments. Under field conditions, sorghum crops often have limited water availability and are exposed to rapidly fluctuating light intensities, which influences both photosynthesis and stomatal behaviour. Our results highlight a tight coupling between photosynthetic rate (A) and stomatal conductance (g_s) even under dynamic light conditions that results in steady intrinsic water use efficiency (W_i). This was mainly due to rapid stomatal responses, with the majority of sorghum accessions responding within ≤5 min. The maintenance of the ratio of the concentration of CO_2 inside the leaf (C_i) and the surrounding atmospheric concentration (C_a) over a large range of accessions suggests high stomatal sensitivity to changes in C_i, that could underlie the rapid g_s responses and extremely close relationship between A and g_s under both dynamic and steady-state conditions. Therefore, sorghum represents a prime candidate for uncovering the elusive mechanisms that coordinate A and g_s, and such information could be used to design crops with high A without incurring significant water losses and eroding W_i.

Keywords: Dynamic light, photosynthesis, photosynthetic induction, *Sorghum bicolor*, speed of stomata, stomatal anatomy, stomatal conductance, water use efficiency.

Introduction

Improvements to crop varieties via breeding, along with improved farming practices, have led to the yields of major crops increasing dramatically since the start of the green revolution of the 1960s (Pingali, 2012; Ort and Long, 2014). The majority of these increases were brought about by advances in agricultural practices and the introduction of dwarf varieties that reduced lodging, enhanced light capture, and improved harvest index [a measure of the ratio of harvestable produce/ yield (e.g. grain) relative to the crop biomass] (Ray *et al.*, 2013; Long *et al.*, 2015). Breeding practices largely assumed that crops can be grown under ideal conditions, and therefore water requirements and nutrient uptake to date have not been the focus of breeding efforts, and, for this reason, few improvements have been made (Pingali, 2012; Ort and Long, 2014). As

such, alongside the near-tripling of crop yield, there has been a comparable increase in agricultural water demand (Pingali, 2012; Ort and Long, 2014). Currently, >80% of the world's fresh water is used in agriculture (WWAP, 2015; D'Odorico *et al.*, 2020) and, as fresh water becomes less readily available due to diminishing groundwater supplies (Dalin *et al.*, 2017), this percentage could be pushed even higher (Dai, 2013; Karmakar *et al.*, 2017; Spinoni *et al.*, 2018). Furthermore, the predicted rise in global temperatures by as much as 2 °C will lead to more sporadic rainfall worldwide, with a declining frequency of precipitation predicted (Dai, 2013; Karmakar *et al.*, 2017; Spinoni *et al.*, 2018; IPCC, 2022), therefore water availability presents one of the main challenges for agriculture in the near future (Leakey *et al.*, 2019). Enhancing the photosynthetic performance of current crop varieties without an increase in water use, as well as increasing the utilization of less common crop species, are pivotal steps toward harnessing available water resources more efficiently. These advancements will be instrumental in achieving the necessary crop productivity to meet global demand (Flexas, 2016; FAO *et al.*, 2018; Kayatz *et al.*, 2019; Leakey *et al.*, 2019).

Crops with C_4 photosynthesis possess a carbon-concentrating mechanism (CCM) maintaining high CO_2 concentration near the carboxylation sites of Rubisco, improving the efficiency of photosynthesis and lowering transpiration, especially in high temperature conditions when evaporative demand is high (Pearcy and Ehleringer, 1984). The CCM mechanism tends to reduce diffusional limitations by stomata and decreases water use (Pearcy and Ehleringer, 1984; Way *et al.*, 2014) compared with C_3 crops, highlighting their potential use in future agriculture. Intrinsic water use efficiency (W_i), defined as the photosynthetic rate (A) divided by stomatal conductance to water vapour (g_s), describes the biological control of the balance between CO_2 uptake and water loss, and is generally higher in C_4 compared with C_3 crops (Blum, 2009; Lawson *et al.*, 2010; Lawson and Blatt, 2014). W_i is determined by leaf anatomy (e.g. stomatal size, density, and aperture) and biochemistry (e.g. photosynthesis capacity) and has been selected for in breeding programmes in the past for improved crop yield (Condon *et al.*, 2002, 2004).

In natural environments, changes in the angle of the sun, cloud cover, and shading from overlapping leaves or neighbouring plants mean that plants are continually exposed to rapid changes in light intensities and spectral properties that have major consequences for photosynthetic carbon assimilation (Pearcy, 1990; Chazdon and Pearcy, 1991; Pearcy and Way, 2012). Photosynthetic photon flux density (PPFD)-driven changes in A occur within several tens of seconds to minutes, compared with changes in g_s which can take up to tens of minutes to reach a new steady state (Barradas and Jones, 1996; Lawson and Morison, 2004; Lawson *et al.*, 2010; Vico *et al.*, 2011; McAusland *et al.*, 2016). A slow increase in g_s can limit A, whilst a slow decrease results in a lag between the drop in A and g_s response. The delay between A and g_s can result

in additional water loss for a reduced carbon gain, lowering W_i (Hetherington and Woodward, 2003; Franks and Farquhar, 2007; Brodribb *et al.*, 2009; Lawson *et al.*, 2010, 2012; Vico *et al.*, 2011; Drake *et al.*, 2013; McAusland *et al.*, 2016). As W_i is determined by both A and g_s, it is important to consider the impact that both parameters can have on W_i. Although high W_i is desirable, this should not be at the expense of A, and therefore g_s rates that are more in line with mesophyll demands for CO_2 should promote higher A and maintain W_i; however, this is only true if stomatal responses to changing conditions are not too slow (McAusland *et al.*, 2016; Lawson and Vialet-Chabrand, 2019). Although species specific, sluggish stomatal responses limit photosynthesis by ~10% (McAusland *et al.*, 2016) and reduce W_i by 20% (Lawson and Blatt, 2014; De Souza *et al.*, 2020; Acevedo-Siaca *et al.*, 2021). Increasing the speed of stomatal responses has therefore become a key target for improved A and W_i (Lawson and Blatt, 2014; Qu *et al.*, 2016; Lawson and Vialet-Chabrand, 2019; Papanatsiou *et al.*, 2019). The significant variation known to exist in stomatal kinetics (Vico *et al.*, 2011; Lawson *et al.*, 2012; Drake *et al.*, 2013; McAusland *et al.*, 2016; Faralli *et al.*, 2019b; Eyland *et al.*, 2021) could be used to identify the underlying genetic variation that influences the speed of stomatal responses, an unexploited target for improving photosynthesis and/or W_i (Faralli *et al.*, 2019b). Qu *et al.* (2020), for example, applied a genome-wide association study (GWAS) and successfully identified a candidate gene (an Na^+/H^+ tonoplastic antiporter OsNHX1) that regulated the speed of stomatal closure.

Sorghum (*Sorghum bicolor* L. Moench) is the second most important C_4 crop globally (USDA, 2022), grown as a traditional, rain-fed, staple grain crop in semi-arid regions with high air and soil surface temperatures and low soil quality, environments in which C_3 crops struggle to thrive (Rao *et al.*, 2006). Recently, variations in anatomical features such as leaf width and stomatal density have been shown to drive differences in W_i in a range of sorghum accessions (Pan *et al.*, 2022; Al-Salman *et al.*, 2023). In these studies, a strong correlation between A and g_s was reported that in most C_3 plant species disappears under fluctuating light environments (Lawson *et al.*, 2012; McAusland *et al.*, 2016; Faralli *et al.*, 2019a, b). The mechanism coordinating A and g_s in C_3 plants is elusive and is thought to depend on a positive feedback loop controlling stomatal aperture based on mesophyll photosynthetic signal (Lawson *et al.*, 2014, 2018), with C_i having long been proposed as the signal coordinating A and g_s (Farquhar *et al.*, 1978; Vialet-Chabrand *et al.*, 2021). Furthermore, many studies have reported that changes in stomatal aperture result in a constant ratio between the concentration of CO_2 inside the leaf (C_i) and the surrounding atmospheric concentration (C_a) (C_i:C_a ratio; Ball *et al.*, 1987; Mott, 1988). This is an appealing prospect as C_i is determined by mesophyll consumption of CO_2 and the flux of CO_2 into the leaf, which is controlled by stomatal conductance (Lawson *et al.*, 2018). However, several studies have

suggested that stomatal responses to C_i are insufficient to account for the changes observed in g_s in response to light (Raschke, 1975; Sharkey and Raschke 1981; Farquhar and Sharkey, 1982). More recent studies have also demonstrated g_s responses to light when C_i was held constant (Messinger *et al.*, 2006; Lawson *et al.*, 2008), suggesting that C_i cannot be the only signal. However, most of these investigations have been performed on C_3 plants, and the mechanism coordinating this relationship may be different in C_4 plants due to the CCM leading to different stomatal behaviour under fluctuating light conditions.

In this study, we assessed natural variation in stomatal and photosynthetic traits and W_i in 43 accessions of sorghum from 16 countries across three continents (Supplementary Table S1). Using this information, one of our main questions was: what is the the dynamic coordination between A and g_s and how does this impact W_i under fluctuating light intensity in a C_4 crop such as sorghum? C_4 crops possess a lower maximum g_s due to their lower stomatal size and density (Taylor *et al.*, 2012) which potentially influences their rapidity of response (McAusland *et al.*, 2016).

Materials and methods

Plant material used in this study

Seed material for the 43 accessions of sorghum (*Sorghum bicolor*) used in this study were kindly provided by Dr Alison Bently (NIAB, Cambridge), Dr Dagmar Janovská (Crop Research Institute, Prague), and Dr Jana Kholova and Dr Sunita Choudhary (ICRISAT, Hyderabad). A full list of accessions used can be found in Supplementary Table S1. Further information on IS lines can be found at www.genesys-pgr.org and on EC lines in Brahmi *et al.* (2015). These accessions include: (i) a range of traditional cultivars or landraces which have been grown as traditional crops in their native region; (ii) advanced or improved cultivars that are the product of modern breeding programmes; and (iii) breeding and research material with notable traits which make them useful parental lines for breeding programmes or notable outliers for research (https://glis.fao.org/glis/).

Growth conditions

Sorghum seed were initially sown on damp tissue paper and stored in the dark at 26 °C for 5 d to induce germination. Healthy seedlings were then transplanted to pots containing peat-based compost (Levingtons F2S, Everris, Ipswich, UK). Plants were grown under controlled conditions in a controlled-environment room, with a constant temperature of 26 °C. Humidity was maintained above 60% using a Trotec B400 humidifier (Trotec, Heinsberg, Germany). Plants were grown under a 10 h:14 h light:dark cycle with daytime lighting maintained at 1000 μmol m^{-2} s^{-1} of full-spectrum white light provided by either LightDNA-8 (Valoya, Helsinki, Finland) or DYNA (Heliospectra, Gothenburg, Sweden) LED grow-lights. Plants were grown in individual pots that were randomly distributed and rotated every 2 d. Plants were watered as required to maintain sufficient soil moisture, with supplemental nutrients provided with weekly application of Hoagland's solution (Hoagland and Arnon, 1950). Before testing, plants were grown to the fifth-leaf stage of growth, which typically took 3–5 weeks. All measurements were taken on the youngest fully expanded primary leaf at the time of testing.

Infra-red gas exchange measurements of photosynthesis

Gas exchange parameters were measured on the youngest fully expanded leaf using a Li-6400 or Li-6800 infrared gas analyser (Li-Cor, Lincoln, NE, USA). For all gas exchange experiments in this study, the internal CO_2 concentration of the leaf cuvette (C_a) was set to 400 μmol mol^{-1}, leaf temperature to 26 °C, and relative air humidity within the cuvette to 60%.

When measuring the response of A to PPFD (A/Q response curves), leaves were initially acclimated under a light irradiance above saturation (2000 mmol m^{-2} s^{-1}) until net photosynthetic CO_2 assimilation (A) had stabilized, at which point the first data point was recorded. PPFD was then decreased in 12 steps (2000, 1500, 1250, 1000, 750, 500, 300, 200, 100, 50, 20, and 0 mmol m^{-2} s^{-1}), with a new recording being taken at each new light level once A had reached a new steady state (typically 1–3 min per step). Data were fitted to a rectangular hyperbola plot of the Michaelis–Menten equation in Rstudio (RStudioTeam, 2020) as previously described in Stevens *et al.* (2021). The initial slope of these modelled curves was used to calculate the maximum apparent quantum yield of net carbon assimilation (QY) for each accession; these values were then compared using a one-way ANOVA using the aov function in Rstudio. Statistically significant differences ($P{\leq}0.05$) were then grouped using a Tukey's post-hoc test.

The response to a rapid increase in PPFD (step change response to light) was measured by first allowing A to stabilize at a PPFD of 100 mmol m^{-2} s^{-1}. Once a steady state was reached, measurements were taken every 10 s for 5 min in order to determine baseline parameters at low light. PPFD was then increased to 1000 mmol m^{-2} s^{-1} and further readings were taken every 10 s for 30 min. Data were fitted in Rstudio (RStudioTeam, 2020), using the model presented in McAusland *et al.* (2016). The time constant for the assimilation rate (τ_{ai}) and stomatal opening (τ_i) were calculated using the excel macro provided in Vialet-Chabrand *et al.* (2017c). A one-way ANOVA was used to assess differences between accessions and, where a significant difference was found, a Tukey's post-hoc test was used to pool accessions into statistically separable groupings.

Measurement of stomatal anatomical characteristics

After gas exchange measurements were completed, stomatal impressions were taken from the abaxial and adaxial leaf surfaces of the same leaf using Xantopren L blue silicone impression material and hardener (Beyer Dental, Leverkusen, Germany) utilizing the method described in Weyers and Johansen (1985). Impression material was allowed to dry fully before being removed from the leaf, after which clear nail varnish was applied to the impression in order to produce a positive replica, which was removed using clear sticky tape and applied to a microscope slide. Light microscopy images were taken using an SC500 5MP microscope digital camera (Swift Optical Instruments, Texas, USA) fitted to a Leica ATC 2000 compound microscope (Leica Microsystems, Wetzlar, Germany) at ×10 objective magnification. The ×10 magnification images were used to take stomatal density measurements in ImageJ (Schneider *et al.*, 2012).

A separate group of plants from 10 selected accessions (EC884904, IS1054, IS10876, IS14556, IS16044, IS24953, IS29472, IS2950, IS23496, and IS36556) were grown and additional impressions were taken. For these plants, in addition to stomatal density, guard cell length and stomatal pore length measurements were made using the tools in the SC500 5MP microscope digital camera's accompanying software, Swift Imaging 3.0 (Swift Optical Instruments). Measurements were made on live images at ×20 objective magnification and exported to Microsoft Excel for further analysis. Maximum anatomical stomatal conductance (anatomical g_{smax}) was calculated from these characteristics using the equation by Dow *et al.* (2014):

$$\text{Anatomical } g_{\text{smax}} = \frac{(d \times \text{SD} \times a_{\text{max}})}{\left(v \times \left(l + \left(\frac{\pi}{2} \right) \times \sqrt{\left(\frac{a_{\text{max}}}{\pi} \right)} \right) \right)}$$

Where d is the diffusivity of water in air (24.6×10^6 m^2 s^{-1} at 25 °C; Dow and Bergmann, 2014) and v is the molecular volume of air (24.4×10^3 m^3 mol^{-1} at 25 °C and 101.3 kPa (Dow and Bergmann, 2014). a_{max}, the maximal stomatal pore area (μm^2), was calculated from the measured pore length, assuming that stomatal pores are elliptical, with a major axis equal to the pore length and the minor axis estimated at half the pore length (McElwain *et al.*, 2016). Stomatal pore depth, l (μm) was estimated as a quarter of the guard cell length.

Statistical analyses of stomatal characteristics were performed in Rstudio (RStudioTeam, 2020). A one-way or two-way ANOVA was used to analyse single-factor or two-factor differences, respectively. Where a significant difference was identified, a Tukey's post-hoc test was performed to group factors by significance.

Results

Photosynthetic and stomatal responses to light intensity

To identify differences in the CO$_2$ assimilation rates (A; Fig. 1A) and stomatal conductance to water vapour (g_s; Fig. 1B) between the 43 tested accessions (Supplementary Fig. S1A, B), we examined A and g_s as a function of light intensity. Ten examples shown in Fig. 1A and B illustrate the resulting light response curves for A and g_s, selected to represent the full range of responses observed. As expected, A initially increased linearly with increasing light intensity before saturating and plateauing at intensities between 500 μmol m^{-2} s^{-1} and 800 μmol m^{-2} s^{-1}. Interestingly g_s showed a similar response pattern to that described for A. As light intensity was changed every 2–3 min, these experiments also provide information on the speed of the dynamic responses of both A and g_s to changing light intensity. As a result of the similar patterns of A and g_s, the $C_i:C_a$ ratio in all accessions was maintained fairly constant (~ 0.25–0.35) at all light intensities apart from those below 250 μmol m^{-2} s^{-1} (Supplementary Fig. S1C).

The initial slope of the light response curves was used to calculate the maximum apparent quantum yield of CO$_2$ assimilation (QY; Fig. 1C) whilst the plateau provided a measure of the light-saturated rate of CO$_2$ assimilation (A_{sat}; Fig. 1D) (and photosynthetic capacity) for each sorghum accession. The QYs of the 43 tested accessions were variable and can broadly be placed into five, heavily overlapping statistical groups (a–e) (Fig. 1C). The accession with the highest average maximum apparent quantum yield, IS36556, a traditional cultivar from Nigeria, had a significantly higher apparent quantum yield than the 12 lines with the lowest QYs. It should be noted that no individual cultivar observed stood alone as statistical anomaly, with all being statistically similar to at least 27 other cultivars, which was also the case for the accession with the lowest average QY, IS5720 (a traditional cultivar from India). A_{sat} also revealed large differences between sorghum accessions (Fig. 1D).

These data split our accessions into 10 statistical groups (a–j), with IS36556 and IS5720 also having the highest and lowest A_{sat}, respectively. When combining data for all accessions, A_{sat} correlated strongly with maximum apparent quantum yield ($R=0.94$, $P<2.2$e-16; Supplementary Fig. S1D).

A strong positive correlation (regression coefficient for all tested accessions $R>0.96$, P-values <5.9e-07) was observed between g_s and A at all irradiances from 0 to 2000 μmol m^{-2} s^{-1} (Fig. 2; Supplementary Fig. S2A). It should be noted that a saturation of A can be seen in some accessions at maximal g_s. In the 10 selected accessions, the regression formulae of these relationships range from IS16044 ($y= -1.7 + 200x$) to IS36556 ($y= -17 + 220x$), illustrating near identical slopes for these 10 accessions. While, typically, the linearity of this correlation indicates a relatively stable W_i, the variation in g_s at low A values suggests differences in W_i between accessions (Fig. 2). It is also apparent from these relationships that the cultivars with the lowest g_s values tend to have lower light-saturated rates of photosynthesis (Fig. 2). For example, IS4556 generally has a higher W_i than EC844904, at the same A (due to lower g_s values). However, at saturating light, IS4556 A_{sat} is significantly lower (~15μmol m^{-2} s^{-1}) than that of EC844904 (~35 μmol m^{-2} s^{-1}). Plotting A_{sat} against g_s under saturating light intensities (g_{ssat}; calculated from the plateau of the data shown in Fig. 1B) for each accession (Fig. 3) also reveals a very strong correlation between these parameters across all 43 accessions ($R=0.99$, $P<2.2$e-16).

Speed of responses to a step increase in irradiance varies between Sorghum accessions

Sorghum plants exposed to a step increase in light intensity from 100 μmol m^{-2} s^{-1} to 1000 μmol m^{-2} s^{-1} showed a typical hyperbolic response in both A (Fig. 4A) and g_s (Fig. 4B). However, significant variation was observed in the final A and g_s values between the different cultivars, with values ranging from 32.95 μmol m^{-2} s^{-1} (IS36556) to 12.74 μmol m^{-2} s^{-1} (IS16044) for A, and 0.21 mol m^{-2} s^{-1} (IS36556) to 0.07 mol m^{-2} s^{-1} (IS23496) for g_s. Visualizing the responses in the 10 selected lines, it is clear that the responses of A to changing irradiance were similar to the g_s responses for each accession. This is further illustrated in the relatively stable C_i values in the majority of the 10 accessions observed during this kinetic response (Supplementary Fig. S3).

In order to parameterize these response kinetics, we used the model presented in McAusland *et al.* (2016) from which time constants for A (τ_{ai}; Fig. 4C; Supplementary Fig. S4A) and g_s (τ_i; Fig. 4D; Supplementary Fig. S4B) were determined for each of our accessions. Values for τ_{ai} (Fig. 4C) ranged from 92 s to 1235 s and could be separated into two statistically significant groups (a and b), while τ_i (Fig. 4D) ranged from 42 s to 1062 s and fitted into three significant but overlapping groups (a–c). IS23496, a traditional cultivar from Ethiopia, was the only accession observed to fit into group 'a' for τ_{ai} and τ_i, with
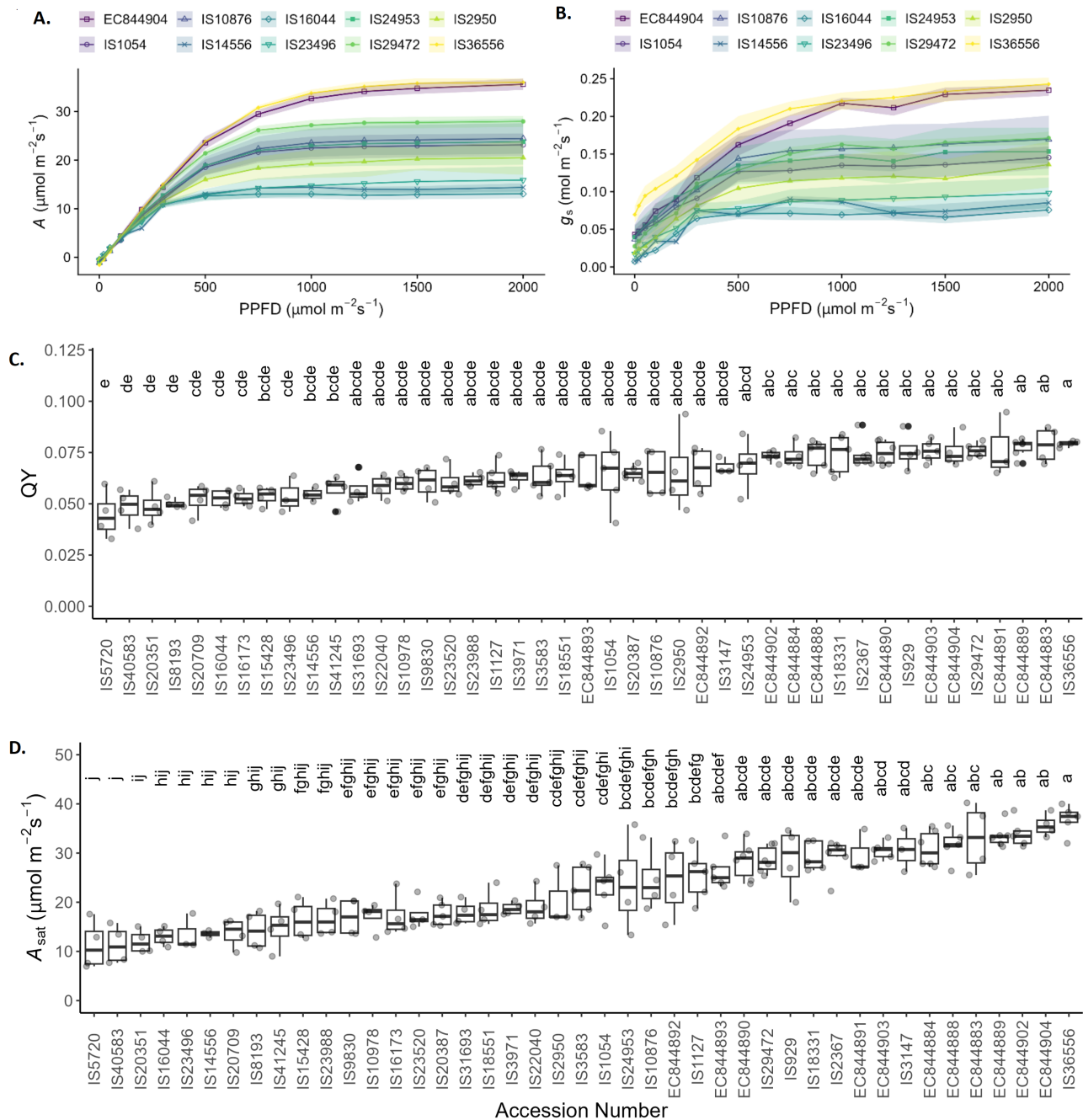
Fig. 1. The effect of light on photosynthetic and stomatal parameters. Light responses of sorghum plants showing (A) CO_2 assimilation rate (*A*) and (B) stomatal conductance to water (g_s) in 10 representative accessions under a range of PPFD irradiance intensities from 0 to 2000 µmol m^{-2} s^{-1}. (C) Maximum apparent quantum yield of net carbon assimilation (QY) for 43 sorghum accessions calculated from the initial slope of the *A*/PPFD curves for each accession. Accession numbers in (C) are ordered from lowest to highest mean QY. (D) Photosynthetic CO_2 assimilation at 2000 µmol m^{-2} s^{-1} (A_{sat}) of 43 sorghum accessions. Accession numbers are ordered from lowest to highest mean A_{sat}. In (C) and (D), colours indicate the biological status of the accession as shown in Supplementary Table S1, and letters indicate significantly different groupings of ANOVA results ($P \leq 0.05$) calculated using a Tukey's test. *n*=3–8. The shaded ribbon represents the SE around the mean.

a significantly slower response for both *A* and g_{sw} to the step increase in irradiance compared with all other cultivars examined. While τ_{ai} and τ_i did not always align on an accession-by-accession basis (Supplementary Fig. S4), when τ_{ai} and τ_i for all cultivars were plotted against each other (Supplementary Fig.

S5), a strong linear correlation was observed (*R*=0.61, *P*<0.05). Despite the synchronicity of the rapidity of response, τ_{ai} and τ_i were not correlated to steady-state g_s and *A* values. It is noteworthy that parameters describing the initial and final g_s and *A* values during photosynthesis induction were significantly
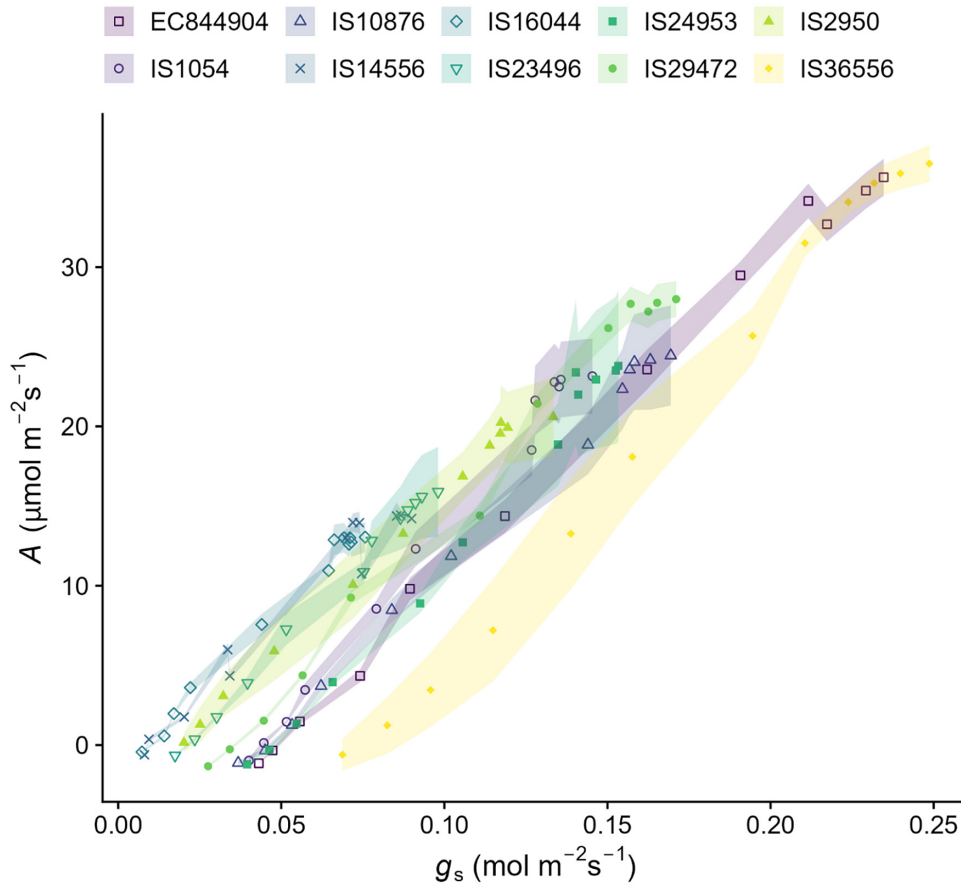
Fig. 2. Rate of change of CO_2 assimilation rate (*A*) relative to stomatal conductance to water (g_s) in response to changes in PPFD irradiance intensities from 0 to 2000 µmol m^{-2} s^{-1}. Data are shown from 10 representative accessions. Points indicate the mean average of 4–8 plants, and ribbons indicate the SE.

intercorrelated ($P<0.05$), with low initial values leading to low final values.

Intrinsic water use efficiency under steady-state irradiance

The kinetic responses of W_i (A/g_s) were determined from the data collected from the step increase in irradiance (see Fig. 4). As the kinetic responses were relatively stable over time (see Supplementary Fig. S6) and differences were only really apparent at 100 µmol m^{-2} s^{-1} and 1000 µmol m^{-2} s^{-1} PPFD, steady-state W_i was determined from the last 5 min at each light intensity (Fig. 5; Supplementary Fig. S7A).

W_i varies greatly between the 10 selected accessions at both 100 µmol m^{-2} s^{-1} and 1000 µmol m^{-2} s^{-1} (Fig. 5). W_i at 1000 µmol m^{-2} s^{-1} can be grouped into six heavily overlapping statistical groups within these 10 cultivars, with IS23496 having the highest average W_i at 1000 µmol m^{-2} s^{-1} and IS36556 having the lowest. At 100 µmol m^{-2} s^{-1}, there are four statistical groups (a–d), and IS16044 has the highest average W_i; the lowest average W_i at 100 µmol m^{-2} s^{-1} was again observed in IS36556 and EC844904.

When assessing all 43 accessions (Supplementary Fig. S7A), W_i at 1000 µmol m^{-2} s^{-1} light exposure was also significantly greater than at 100 µmol m^{-2} s^{-1} ($P<0.05$) in all observed accessions except IS10978, a traditional cultivar from the USA ($P=0.511$). Eleven heavily overlapping statistical groups of W_i (a–k) at 100 µmol m^{-2} s^{-1} and 13 (a–m) at 1000 µmol m^{-2} s^{-1} were identified. The accession with the highest average W_i at 1000 µmol m^{-2} s^{-1} was IS40583 (BTx623), a research line from the USA, which had a statistically higher W_i than 30 other accessions. At 100 µmol m^{-2} s^{-1}, however, while IS40583 still had a high W_i, fitting into groups 'a–d', its W_i was only statistically greater than that of 16 other accessions. Meanwhile the accession with the lowest W_i at 1000 µmol m^{-2} s^{-1}, the Nigerian landrace variety IS36556, was only significantly lower than 27 of the 43 tested accessions but the W_i of IS36556 at 100 m^{-2} s^{-1} was significantly lower than that of 36 of the 43 accessions. By directly comparing the W_i at 100 µmol m^{-2} s^{-1} with that at 1000 µmol m^{-2} s^{-1} for all measured accessions (Supplementary Fig. S7B), a significant correlation between these parameters was seen ($R=0.49$, $P=0.00077$), showing
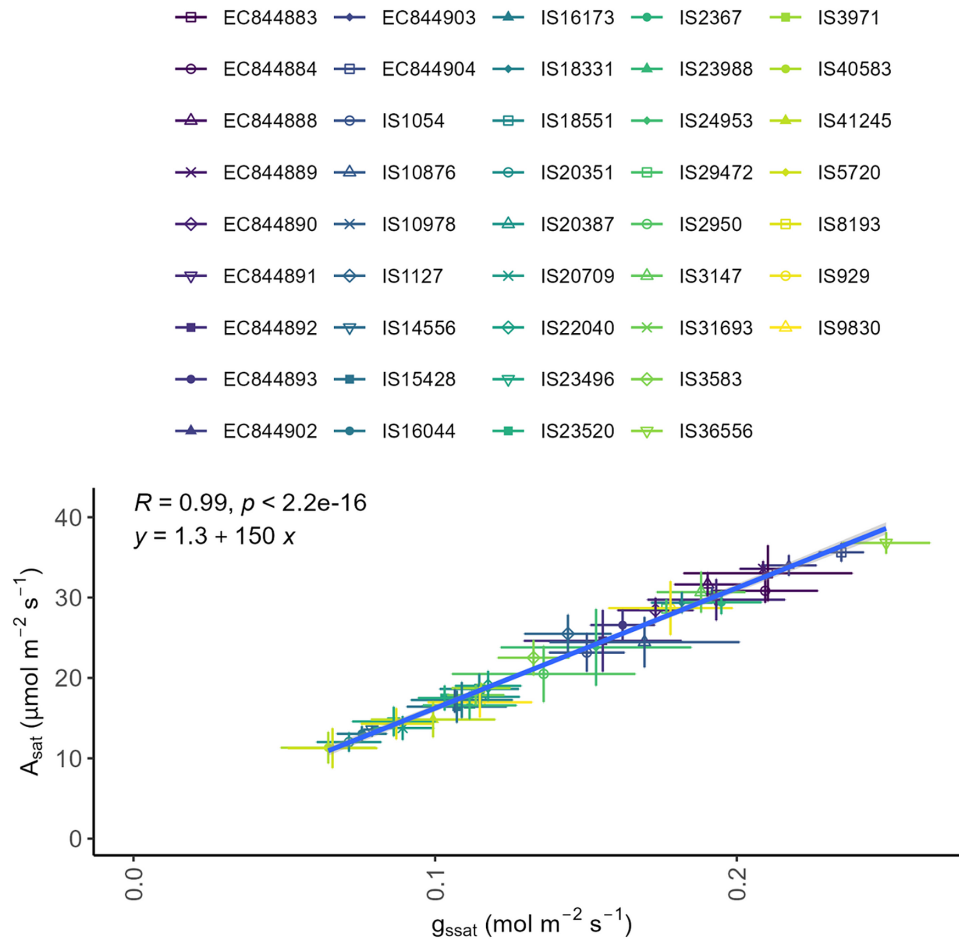
Fig. 3. Light-saturated rate of photosynthetic CO_2 assimilation (A_{sat}; *A* at 2000 µmol m^{-2} s^{-1}) relative to stomatal conductance under saturating light (g_{ssat}; g_s at 2000 µmol m^{-2} s^{-1}) for each tested sorghum accession. Points indicate mean average values for accessions as indicated by colour. Error bars indicate the SE of the mean, *n*=3–8. The line represents *R*=0.99, *P*<2.2e-16 with a regression formula of *y*=1.3 + 150*x*.

that accessions with higher W_i tended to have consistently greater efficiency at both high and low light than those with lower W_i.

Stomatal anatomy of sorghum varies by accession and by leaf surface

Stomatal density (SD) was measured on the abaxial (AB) and adaxial (AD) surface of all 43 sorghum accessions (Fig. 6A) and showed a range of SD values from 185 stomata mm^{-2} (IS31693) to 51 mm^{-2} (IS10978 and IS23520) for the AB surface and 121 mm^{-2} (IS18331) to 28 mm^{-2} (IS3583 and IS23520) for the AD surface. The accession with the highest average SD across both leaf surfaces was EC844902, an accession from Mali, with an average of 106.5 stomata mm^{-2}, which was significantly higher than the four accessions with the lowest SD; IS3583 (65.0 mm^{-2}), IS23520 (64.8 mm^{-2}), IS10978 (64.6 mm^{-2}), and IS20709 (64.1 mm^{-2}). At this resolution of SD measurement, the average SDs of the remaining 38 accessions were statistically comparable with those of all 43 tested accessions.

SD was generally higher on the AB compared with all AD surface for all accessions; however, these differences were only significant (*P*<0.05) for 11 lines (Fig. 6A). In order to further analyse and validate these findings for the 10 selected lines, a more in-depth analysis was performed on stomatal anatomical features, including SD measured from nine fields of view per leaf surface per plant for six plants per accession (Fig. 6B) (where previously a single field of view had been measured per surface per plant for 2–6 plants per accession) and guard cell length and stomatal pore length, which were each measured from nine stomata per leaf surface per plant for six plants per accession. These data were used to calculate maximum anatomical stomatal conductance (anatomical g_{smax}) for each leaf surface (Fig. 6C).

When comparing SD alone in these selected accessions (Fig. 6B), sorghum in nine of the 10 accessions again had significantly higher SD on the AB than on the AD leaf surface (*P*<0.0001). In this case, only EC844904 was observed to have no significant difference between the AB and AD leaf surface, with a statistically similar SD on each (*P*>0.05). Average SD
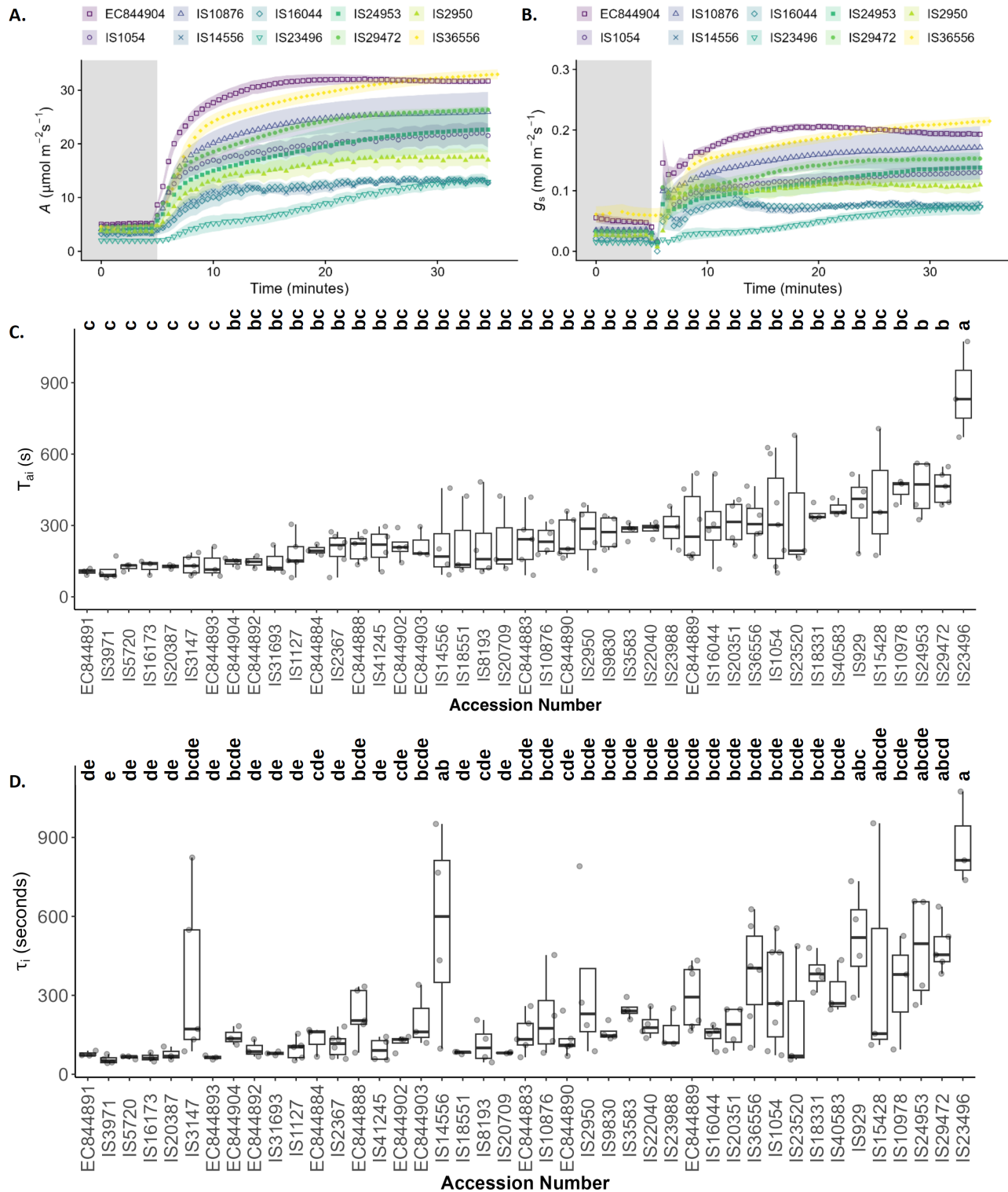
Fig. 4. Stomatal and photosynetic kinetic responses. Temporal responses to a rapid increase in PPFD irradiance from 100 µmol m^{-2} s^{-1} (shaded area) to 1000 µmol m^{-2} s^{-1} showing changes in (A) CO$_2$ assimilation rate (*A*) and (B) stomatal conductance to water (*g$_s$*) in 10 representative sorghum accessions. Data from this protocol were used to calculated time constants of the (C) light-saturated rate of carbon assimilation (τ$_{ai}$) and (D) stomatal opening (τ$_i$) in seconds, shown here for each tested sorghum accession. Accession numbers in (C) and (D) are ordered from the lowest to highest mean τ$_{ai}$. In (C) and (D), colours indicate the biological status of the accession as shown in Supplementary Table S1, and letters indicate significantly different groupings of ANOVA results (*P*≤0.05) calculated using a Tukey's test. The shaded ribbon represent the SE around the mean.
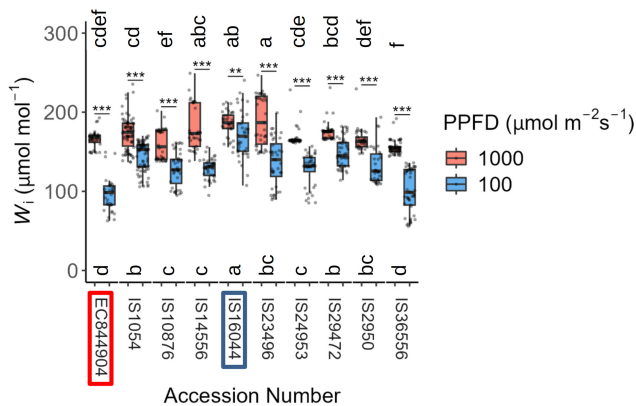
Fig. 5. Changes in intrinsic water use efficiency (W_i) in response to PPFD irradiance. Average W_i measured every 30 s for 5 min of dark-adapted plants exposed to 100 μmol m^{-2} s^{-1} of light (blue boxplots) compared with average W_i measured every 30 s for 5 min after 30 min of exposure to 1000 μmol m^{-2} s^{-1} of PPFD irradiance (red boxplots). The graph shows data from 10 representative sorghum accessions. Asterisks (*) above accessions indicate a significant difference between plants treated with 100 μmol m^{-2} s^{-1} and 1000 μmol m^{-2} s^{-1} for the given accession calculated by ANOVA (***$P<0.0001$, **$P=0.001-0.01$, *$P=0.01-0.05$). Letters indicate significantly different groupings of ANOVA results ($P≤0.05$) of accessions for plants exposed to 100 μmol m^{-2} s^{-1} (letters below the boxplots) or 1000 μmol m^{-2} s^{-1} (letters above the boxplots) of PPFD irradiance. Groupings were calculated using a post-hoc Tukey's test, $n=4-8$. Highlighted accession numbers identify the lowest g_{smax} (red box) and the second lowest g_{smax} (blue box).

across the combined leaf surfaces in Fig. 6B can be separated into five groups amongst these 10 plants. The highest stomatal densities are seen in the Lesothan landrace variety, IS29472, and the American breeding line IS2950, both of which are statistically comparable with each other and have a significantly greater SD than all other accessions. IS10876, a Nigerian landrace, has the lowest average SD of the observed accessions, with a statistically lower average SD than all but two of the other accessions. There was no relationship between stomatal size and density.

Anatomical g_{smax} showed that sorghum typically had a greater potential g_s on the AB leaf surface (Fig. 6C). Eight of the 10 selected lines presented significantly greater ($P<0.0001$) anatomical g_{smax} on the AB surface than on the AD surface. EC844904 and IS23496 showed no significantly different anatomical g_{smax} between surfaces ($P>0.05$). Of these 10 accessions, IS14556, an Ethiopian landrace variety, had significantly higher anatomical g_{smax} over the combined leaf surfaces than all but three other varieties, IS36556, a Nigerian landrace, IS23496, an Ethiopian landrace, and IS2950, a research line from the USA. Pooling the SD data for all of the 43 accessions revealed a strong correlation between AD and AB SD (Supplementary Fig. S8; $R=0.22$, $P=0.048$), showing that the AB SD was typically higher than the AD SD, and an increase in SD on one surface was typically accompanied by an increase on the opposite surface. Leaf anatomical parameters such as SD and guard cell length and pore size were significantly correlated ($P<0.05$) to the g_s and A values reached at the end of a photosynthesis induction (Supplementary Fig. S8). However, these correlations had relatively low R^2, with values ranging from 0.12 to 0.2.

Discussion

As expected, sorghum can operate at low g_s, whilst maintaining relatively high photosynthesis levels compared with C$_3$ plants. The resulting low operating C_i was in a relatively small range of values among accessions and near the edge of what is required for photosynthetic saturation, with values around or even sometimes below the 100–150 μmol mol^{-1} range reported previously (Pearcy and Ehleringer, 1984; Ehleringer and Monson, 1993). Despite similar C_i values, a large diversity in g_s and A was observed in the 43 sorghum accessions studied here, and an extremely strong correlation and synchronicity between A and g_s at different light levels was clearly evident. Our results highlight a tight control of gaseous exchange in both dynamic and steady-state conditions in sorghum, with implications for water use efficiency. Accessions with the greatest A displayed the highest g_s values, and vice versa, in both steady and non-steady-state conditions (Figs 1–3). These findings provide new insights into the coordination of A and g_s, and potential novel targets for manipulation to increase crop production.

Whilst significant diversity in photosynthetic capacity including the maximum quantum yield (Fig. 1C) and light-saturated rate of photosynthesis (A_{sat}) (Fig. 1D) was observed, what was particularly interesting and surprising was the near identical patterns of behaviour in g_s in response to changing irradiance as those recorded for A (Fig. 1A, B). Light response curves are most often utilized to determine differences in photosynthetic performance, and measurements are carried out rapidly, with A typically recorded ~1–2 min after a change in light intensity in order to ensure that stomata remain open and do not influence the measurements (Parsons *et al.*, 1998). In the 10 accessions selected, the response of A and g_s was almost identical, with rapid adjustment in stomatal aperture, within 2 min of changing irradiance, resulting in a highly significant and tight correlation between A and g_s (Fig. 2) in all accessions (Supplementary Fig. S2). It is well established that there is a close correlation between A and g_s (Wong *et al.*, 1979) [which forms the basis of the Ball, Woodraw, Berry model (Ball *et al.*, 1987)] and that such synchronous behaviour optimizes carbon gain to water loss (Buckley, 2017). However, although these relationships are often conserved, they are not constant and under non-steady-state conditions significant deviation can be seen, often due to relatively slow g_s responses relative to A (Lawson *et al.*, 1998, 2010). Here we have demonstrated near linear relationships between A and g_s in response to dynamic changes in light intensity (Fig. 2) in all accessions, although variation in the absolute values was apparent. This was enabled by the rapid stomatal responses reported here (Fig. 4),
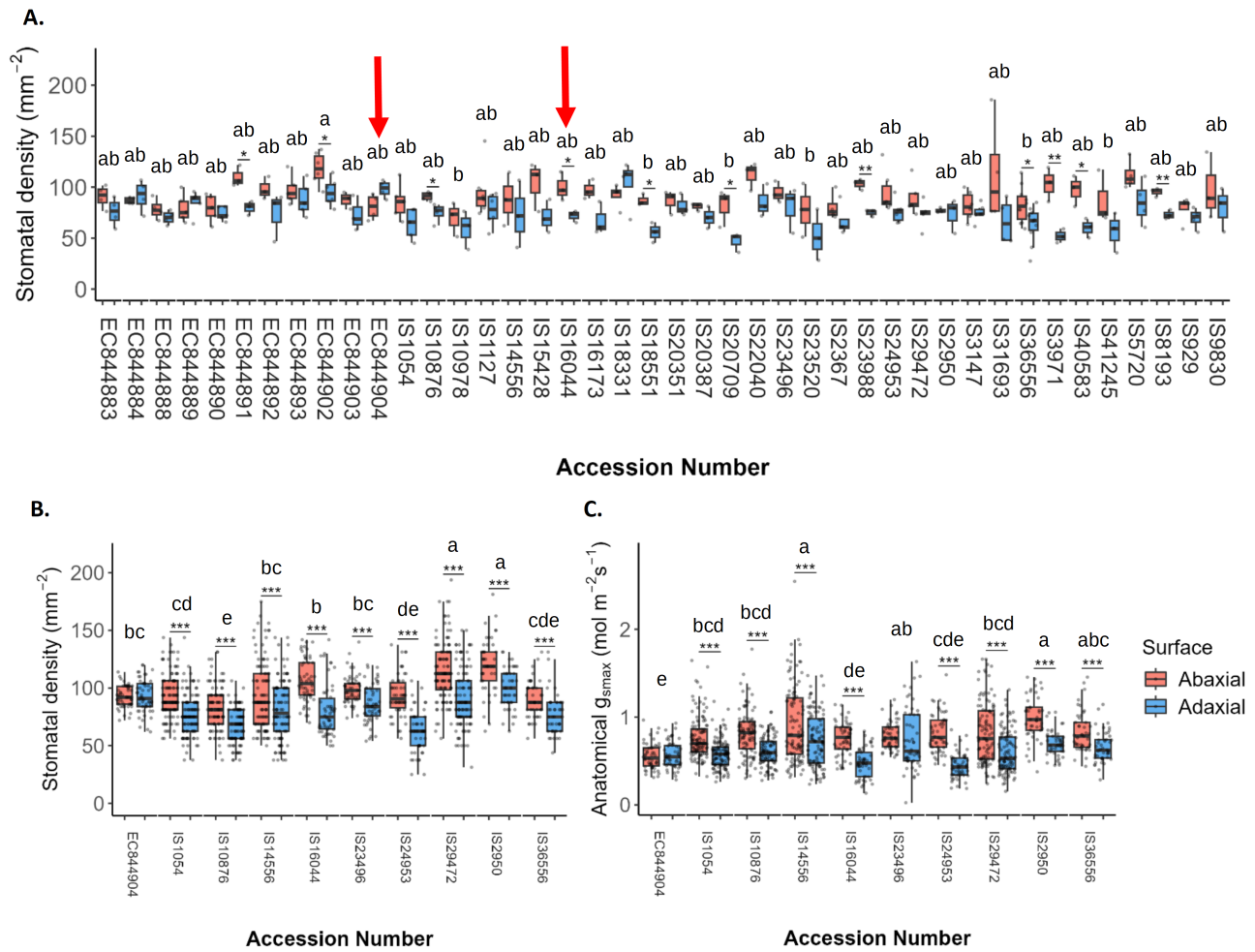
Fig. 6. Variation of stomatal anatomy by leaf surface in sorghum. (A) Stomatal density of all accessions tested in this study measured from one field of view per leaf surface per plant for 2–6 plants per accession. Red arrows indicate accessions with the lowest g_{smax} (EC844904) and the second lowest (IS16044). (B) Stomatal density of 10 representative sorghum accessions measured from nine fields of view per leaf surface per plant for six plants per accession. (C) Maximum anatomical stomatal conductance (anatomical g_{smax}) of 10 representative sorghum accessions calculated from the stomatal densities in (B) and the measured guard cell length and pore length of nine stomata per leaf surface per plant for six plants per accession. In each graph, separate measurements are shown for the abaxial (red) and adaxial (blue) leaf surface of each accession. Asterisks (*) above accessions indicate a significant difference between abaxial and adaxial leaf surfaces for the given accession calculated by ANOVA (***$P< 0.0001$, **$P=0.001$–0.01, *$P=0.01$–0.05). Letters indicate significantly different groupings of ANOVA results ($P\leq0.05$) of accessions based on combined abaxial and adaxial values for each accession calculated using a Tukey's test, $n=6$.

which also helped maintain a constant W_i (Supplementary Fig. S6) under changing irradiance. Here we demonstrated an extremely tight ($R^2=0.99$) coupling of g_{ssat} and A_{sat} (Fig. 3), along with a maintenance of C_i, illustrating an impressive control of gaseous fluxes via stomata that are linked directly to mesophyll CO_2 demands, enabling sorghum to maintain high steady-state W_i without compromise to A.

The observed diversity of g_s and A values whilst maintaining a tight relationship suggests that there is a common signal to which stomata respond rapidly, which facilitates high water use efficiency. Such a strong relationship between g_s and A has often been interpreted as a diffusional constraint on photosynthesis; however, it could also result from a strong signal regulating g_s to maintain saturating C_i while limiting water

loss. Stomatal conductance in C_4 plants is usually not limiting in non-stressed plants as long as operational C_i is allowed to reach saturation (Bunce, 2005; Ghannoum, 2008). The assumption of a signal coordinating A and g_s is supported by the relatively stable and expected C_i:C_a ratios of between 0.3 and 0.4 (Jones, 1983) (Supplementary Fig. S1) and stable C_i values (Supplementary Fig. S3) although these were a little lower than the expected ~100–150 µmol mol^{-1} in some accessions (Pearcy and Ehleringer, 1984; Ehleringer and Monson, 1993).

A number of studies have previously suggested that temporal responses to increasing light intensity lead to a disconnect between A and g_s (Lawson and Blatt, 2014; Kaiser *et al.*, 2016; McAusland *et al.*, 2016; Matthews *et al.*, 2017, 2018; Vialet-Chabrand *et al.*, 2017a, b; De Souza *et al.*, 2020; Yamori

et al., 2020) due to the difference in rapidity of these responses for g_s compared with *A* (McAusland *et al.*, 2016; Qu *et al.*, 2016; Matthews *et al.*, 2017). In C_3 crops, stomatal responses are in general an order of magnitude slower than photosynthetic responses, resulting in diffusive limitation during stomatal opening or unnecessary water loss during stomatal closure (Lawson and Blatt, 2014; McAusland *et al.*, 2016; Faralli *et al.*, 2019b; De Souza *et al.*, 2020). In contrast, our observations displayed significant variation in the response of both *A* and g_s, with dynamic responses that were atypically strongly coordinated in the short term (Fig. 4A, B). The speeds of *A* induction (τ_{ai}) and the rapidity of increase in g_s (τ_i) were <10 min for the vast majority of the lines (Fig. 4D). Although several C_3 cereal crop species have been reported to have rapid stomatal responses, only rice, barley, and Miscanthus have been reported to be this fast in g_s kinetics (see McAusland *et al.*, 2016). In general stomatal opening and closing have been reported to be more rapid in grasses (Franks and Farqhuar 2007; Nunes *et al.*, 2022), which is thought to be due to the relationship between guard and subsidiary cells (Franks and Farqhuar, 2007; Raissig *et al.*, 2017). However, photosynthetic type also plays a role, with C_4 plants reported to be more rapid than C_3 plants (McAusland *et al.*, 2016). Ozeki *et al.* (2022) also demonstrated that rapid stomatal closure contributed to higher water use efficiency in C_4 compared with C_3 *Poaceae* crops. The speed of *A* induction was typically more rapid than for most field crops (McAusland *et al.*, 2016), fruit crops (Zhang *et al.*, 2022), as well as the model Arabidopsis (Burgess *et al.*, 2023). This suggests that sorghum has a mechanism that maintains both the coordination between steady-state *A* and g_s and the extremely tight synchrony of their responses through time. In C_3 crops, different hypotheses have been proposed (Lawson *et al.*, 2014, 2018); there is strong support for a positive feedback loop that controls stomatal aperture based on mesophyll photosynthesis, with C_i potentially coordinating the response (Farquhar *et al.*, 1978; Vialet-Chabrand *et al.*, 2021). A coordination based on C_i would result in a relatively constant W_i as observed in this study. This would suggest an extreme sensitivity of sorghum stomata to internal CO_2 concentration that remains to be tested.

The generally fast stomatal responses observed here lead to a strong correlation between the speed of g_s and the speed of *A*, confirming the importance of the rapidity of stomatal responses in photosynthetic induction (Supplementary Fig. S4) (Long *et al.*, 2022). As stomatal conductance is determined by both anatomical and biochemical features (Hetherington and Woodward, 2003; Franks and Farquhar, 2007), we measured SD on both the AD and AB leaf surface (Fig. 6). As expected, a greater number of stomata were generally observed on the AD surface; however, these differences were not always significant, with 17 of the 43 species having no significant difference in SD between AB and AD surfaces (Fig. 6). Generally, AD and AB SD were correlated (Supplementary Fig. S8), and similar patterns have been observed in wheat, suggesting a common signal that coordinates stomatal anatomy between the two surfaces (Wall *et al.*, 2022), although to date the signal transduction pathway has not been fully elucidated (Santos *et al.*, 2021). Differences in SD between surfaces are well established in amphistomatous leaves (Ticha, 1982), although the impact on functional responses is less well understood (Mott *et al.*, 1982; Mott and O'Leary, 1984; Xiong and Flexas, 2020; Santos *et al.*, 2021; Wall *et al.*, 2022). Anatomical g_{smax} provides a measure of the maximum potential g_s and therefore is indicative of possible functional differences (Lawson *et al.*, 1998; Franks and Farquhar, 2001; Lawson and Morison, 2004; Dow and Bergmann, 2014). All accessions had a low g_{smax} compared with C_3 crops, which is in accordance with previous results (Taylor *et al.*, 2012). EC844904 had the lowest leaf g_{smax}, with IS16044 the second lowest; interestingly, these two accessions also exhibited the lowest and one of the highest leaf W_i values (Fig. 5), illustrating that W_i is strongly influenced by stomatal behaviour. As no correlation was observed between the speed of g_s responses and SD, this suggests that this behaviour was probably not driven by variation in anatomy but supports the idea that stomatal biochemistry and metabolism contribute more to the rapidity of g_s (Lawson and Blatt, 2014). Surprisingly, none of the parameters measured in this study appears to be strongly linked to the country of origin of the accessions, suggesting that development of variability between these accessions was not strongly driven by geographic location.

In conclusion, this study has demonstrated that sorghum displays one of the most rapid stomatal responses in a crop species, with the majority of accessions responding within ≤5 min, and validates the suggestions that stomatal rapidity is greater in C_4 than in C_3 plants (McAusland *et al.*, 2016; Nunes *et al.*, 2022; Ozeki *et al.*, 2022). The strong coordination of *A* and g_s under both steady-state and dynamic conditions with a diversity in absolute values has not previously been reported and implies that a mesophyll signal or C_i tightly regulates stomatal conductance in order to minimize water loss and maximize photosynthesis. Differences in stomatal kinetics and levels reached at each light intensity were not driven by variation in leaf anatomy, but due to functional differences that determine osmoregulation, such as guard cell metabolism or ion channel sensitivity (Blatt and Clint, 1989; Ache *et al.*, 2000; Hosy *et al.*, 2003; Lawson and Blatt, 2014; Lawson *et al.*, 2014; Jezek and Blatt, 2017). Therefore, sorghum represents a prime candidate for uncovering the elusive mechanisms that coordinate *A* and g_s, as well as guard cell traits that permit such rapid g_s responses and using such information to design crops with high *A* without incurring significant water losses and eroding W_i. Ideally, it is advantageous to have crops that have rapid g_s responses, that are closely coupled with mesophyll demands for CO_2 to maximize *A*, water use, and overall crop productivity. The mechanisms that enable sorghum to achieve this could provide as yet unknown targets to improve productivity in both C_3 and C_4 crops.

Supplementary data

The following supplementary data are available at *JXB* online.

Table S1. *Sorghum bicolor* L. Moench accessions used in this study.

Fig. S1. Light response curves and relationship between maximum apparent quantum yield and photosynthetic CO_2 assimilation for the 43 sorghum accessions.

Fig. S2. Rate of change of CO_2 assimilation rate (A) relative to stomatal conductance to water (g_s) in response to changes in PPFD.

Fig. S3. Temporal responses of internal CO_2 concentration (C_i) to increase in PPFD.

Fig. S4. Time constants of carbon assimilation and stomatal opening.

Fig. S5. Association between the rate of induction of carbon assimilation and speed of stomatal opening.

Fig. S6. Temporal response of intrinsic water use efficiency (W_i) to a rapid increase in PPFD irradiance.

Fig. S7. Changes in intrinsic water use efficiency (W_i).

Fig. S8. Matrix representing multiple regressions between modelled parameters describing the rapidity of stomatal and net CO_2 assimilation response and leaf anatomical parameters.

Author contributions

MB, SVC, and TL: designed the experiments; MB, and SVC: performed all physiology experiments, data acquisition, and data analyses; PK: collected stomatal data; MB, AS, SVC, and TL: writing.

Conflict of interest

The authors declare no conflicts of interest.

Funding

Data availability

Data are available on request from the corresponding author.

References

Acevedo-Siaca LG, Dionora J, Laza R, Paul Quick W, Long SP. 2021. Dynamics of photosynthetic induction and relaxation within the canopy of rice and two wild relatives. Food and Energy Security **10**, e286.

Ache P, Becker D, Ivashikina N, Dietrich P, Roelfsema MR, Hedrich R. 2000. GORK, a delayed outward rectifier expressed in guard cells of *Arabidopsis thaliana*, is a K$^+$-selective, K$^+$-sensing ion channel. FEBS Letters **486**, 93–98.

Al-Salman Y, Cano FJ, Pan L, Koller F, Piñeiro J, Jordan D, Ghannoum O. 2023. Anatomical drivers of stomatal conductance in sorghum lines with different leaf widths grown under different temperatures. Plant, Cell & Environment **46**, 2142–2158.

Ball JT, Woodrow IE, Berry JA. 1987. A model predicting stomatal conductance and its contribution to the control of photosynthesis under different environmental conditions. In: Biggins J, ed. Progress in Photosynthesis Research, Vol **4**. Dordrecht: Martinus-Nijhoff Publishers, 221–224.

Barradas VL, Jones HG. 1996. Responses of CO_2 assimilation to changes in irradiance: laboratory and field data and a model for beans (*Phaseolus vulgaris* L.). Journal of Experimental Botany **47**, 639–645.

Blatt MR, Clint GM. 1989. Mechanisms of fusicoccin action: kinetic modification and inactivation of K$^+$ channels in guard cells. Planta **178**, 509–523.

Blum A. 2009. Effective use of water (EUW) and not water-use efficiency (WUE) is the target of crop yield improvement under drought stress. Field Crops Research **112**, 119–123.

Brahmi P, Tyagi V, Yadav SK, Pedapati A, Singh SP, Singh S, Binda PC. 2015. Exotic collections (April–June, 2015). Plant Germplasm Reporter **15**, 1–173. http://www.nbpgr.ernet.in/Downloadfile.aspx?EntryId=7305

Brodribb TJ, McAdam SAM, Jordan GJ, Feild TS. 2009. Evolution of stomatal responsiveness to CO_2 and optimization of water-use efficiency among land plants. New Phytologist **183**, 839–847.

Buckley TN. 2017. Modeling stomatal conductance. Plant Physiology **174**, 572–582.

Bunce JA. 2005. What is the usual internal carbon dioxide concentration in C4 species under midday field conditions? Photosynthetica **43**, 603–608.

Burgess AJ, Retkute R, Murchie EH. 2023. Photoacclimation and entrainment of photosynthesis by fluctuating light varies according to genotype in *Arabidopsis thaliana*. Frontiers in Plant Science **14**, 1116367.

Chazdon RL, Pearcy RW. 1991. The importance of sunflecks for forest understory plants. BioScience **41**, 760–766.

Condon AG, Richards RA, Rebetzke GJ, Farquhar GD. 2002. Improving intrinsic water-use efficiency and crop yield. Crop Science **42**, 122–131.

Condon AG, Richards RA, Rebetzke GJ, Farquhar GD. 2004. Breeding for high water-use efficiency. Journal of Experimental Botany **55**, 2447–2460.

Dai A. 2013. Increasing drought under global warming in observations and models. Nature Climate Change **3**, 52–58.

Dalin C, Wada Y, Kastner T, Puma MJ. 2017. Groundwater depletion embedded in international food trade. Nature **543**, 700–704.

De Souza AP, Wang Y, Orr DJ, Carmo-Silva E, Long SP. 2020. Photosynthesis across African cassava germplasm is limited by Rubisco and mesophyll conductance at steady state, but by stomatal conductance in fluctuating light. New Phytologist **225**, 2498–2512.

D'Odorico P, Chiarelli DD, Rosa L, Bini A, Zilberman D, Rulli MC. 2020. The global value of water in agriculture. Proceedings of the National Academy of Sciences, USA **117**, 21985–21993.

Dow GJ, Bergmann DC. 2014. Patterning and processes: how stomatal development defines physiological potential. Current Opinion in Plant Biology **21**, 67–74.

Dow GJ, Bergmann DC, Berry JA. 2014. An integrated model of stomatal development and leaf physiology. New Phytologist **201**, 1218–1226.

Drake PL, Froend RH, Franks PJ. 2013. Smaller, faster stomata: scaling of stomatal size, rate of response, and stomatal conductance. Journal of Experimental Botany **64**, 495–505.

Ehleringer JR, Monson RK. 1993. Evolutionary and ecological aspects of photosynthetic pathway variation. Annual Review of Ecology and Systematics **1**, 411–439.

Eyland D, van Wesemael J, Lawson T, Carpentier S. 2021. The impact of slow stomatal kinetics on photosynthesis and water use efficiency under fluctuating light. Plant Physiology **186**, 998–1012.

FAO, IFAD, UNICEF, WFP, WHO. 2018. The state of food security and nutrition in the world 2018. Building climate resilience for food security and nutrition. Rome: Food and Agriculture Organization.

Faralli M, Cockram J, Ober E, Wall S, Galle A, Van Rie J, Raines C, Lawson T. 2019a. Genotypic, developmental and environmental effects on the rapidity of Gs in wheat: impacts on carbon gain and water-use efficiency. Frontiers in Plant Science **10**, 492.

Faralli M, Matthews J, Lawson T. 2019b. Exploiting natural variation and genetic manipulation of stomatal conductance for crop improvement. Current Opinion in Plant Biology **49**, 1–7.

Farquhar GD, Dubbe DR, Raschke K. 1978. Gain of the feedback loop involving carbon dioxide and stomata: theory and measurement. Plant Physiology **62**, 406–412.

Farquhar GD, Sharkey TD. 1982. Stomatal conductance and photosynthesis. Annual Review of Plant Physiology **33**, 317–345.

Flexas J. 2016. Genetic improvement of leaf photosynthesis and intrinsic water use efficiency in C_3 plants: why so much little success? Plant Science **251**, 155–161.

Franks PJ, Farquhar GD. 2001. The effect of exogenous abscisic acid on stomatal development, stomatal mechanics, and leaf gas exchange in *Tradescantia virginiana*. Plant Physiology **125**, 935–942.

Franks PJ, Farquhar GD. 2007. The mechanical diversity of stomata and its significance in gas-exchange control. Plant Physiology **143**, 78–87.

Ghannoum O. 2008. C_4 photosynthesis and water stress. Annals of Botany **103**, 635–644.

Hetherington AM, Woodward FI. 2003. The role of stomata in sensing and driving environmental change. Nature **424**, 901–908.

Hoagland DR, Arnon DI. 1950. The water-culture method for growing plants without soil. California Agricultural Experiment Station, Circular **347**.

Hosy E, Vavasseur A, Mouline K, et al. 2003. The *Arabidopsis* outward K^+ channel *GORK* is involved in regulation of stomatal movements and plant transpiration. Proceedings of the National Academy of Sciences, USA **100**, 5549–5554.

IPCC. 2022. Climate Change 2022: impacts, adaptation and vulnerability. In: Pörtner HO, Roberts DC, Tignor M, *et al*., eds. Contribution of working group II to the sixth assessment report of the intergovernmental panel on climate change. Cambridge, UK and New York, NY, USA: Cambridge University Press.

Jezek M, Blatt MR. 2017. The membrane transport system of the guard cell and its integration for stomatal dynamics. Plant Physiology **174**, 487–519.

Kaiser E, Morales A, Harbinson J, Heuvelink E, Prinzenberg AE, Marcelis LF. 2016. Metabolic and diffusional limitations of photosynthesis in fluctuating irradiance in *Arabidopsis thaliana*. Scientific Reports **6**, 31252.

Jones HG. 1983. Plants and microclimate. A quantitative approach to environmental plant physiology. Cambridge: Cambridge University Press.

Karmakar N, Chakraborty A, Nanjundiah RS. 2017. Increased sporadic extremes decrease the intraseasonal variability in the Indian summer monsoon rainfall. Scientific Reports **7**, 7824.

Kayatz B, Harris F, Hillier J, Adhya T, Dalin C, Nayak D, Green RF, Smith P, Dangour AD. 2019. 'More crop per drop': exploring India's cereal water use since 2005. Science of the Total Environment **673**, 207–217.

Lawson T, Blatt MR. 2014. Stomatal size, speed, and responsiveness impact on photosynthesis and water use efficiency. Plant Physiology **164**, 1556–1570.

Lawson T, Kramer DM, Raines CA. 2012. Improving yield by exploiting mechanisms underlying natural variation of photosynthesis. Current Opinion in Biotechnology **23**, 215–220.

Lawson T, Lefebvre S, Baker NR, Morison JIL, Raines CA. 2008. Reductions in mesopyhll and guard cell photosynthesis impacts on the control of stomata to light and CO2. Journal of Experimental Botany **59**, 3609–3619.

Lawson T, Morison JIL. 2004. Stomatal function and physiology. In: Hemsley AR, Poole I, eds. The evolution of plant physiology. Oxford: Academic Press, 217–242.

Lawson T, Simkin AJ, Kelly G, Granot D. 2014. Mesophyll photosynthesis and guard cell metabolism impacts on stomatal behaviour. New Phytologist **203**, 1064–1081.

Lawson T, Terashima I, Fujita T, Wang Y. 2018. Coordination between photosynthesis and stomatal behavior. In: Adams WW **III**, Terashima I, eds. The leaf: a platform for performing photosynthesis. Cham: Springer International Publishing, 141–161.

Lawson T, Vialet-Chabrand S. 2019. Speedy stomata, photosynthesis and plant water use efficiency. New Phytologist **221**, 93–98.

Lawson T, von Caemmerer S, Baroli I. 2010. Photosynthesis and stomatal behaviour. In: Lüttge UE, Beyschlag W, Büdel B, Francis D, eds. Progress in botany Vol. **72**. Berlin, Heidelberg: Springer Berlin Heidelberg, 265–304.

Lawson T, Weyers J, A'Brook R. 1998. The nature of heterogeneity in the stomatal behaviour of *Phaseolus vulgaris* L. primary leaves. Journal of Experimental Botany **49**, 1387–1395.

Leakey ADB, Ferguson JN, Pignon CP, Wu A, Jin Z, Hammer GL, Lobell DB. 2019. Water use efficiency as a constraint and target for improving the resilience and productivity of C_3 and C_4 crops. Annual Review of Plant Biology **70**, 781–808.

Long SP, Marshall-Colon A, Zhu XG. 2015. Meeting the global food demand of the future by engineering crop photosynthesis and yield potential. Cell **161**, 56–66.

Long SP, Taylor SH, Burgess SJ, Carmo-Silva E, Lawson T, De Souza AP, Leonelli L, Wang Y. 2022. Into the shadows and back into sunlight: photosynthesis in fluctuating light. Annual Review of Plant Biology **73**, 617–648.

Matthews JSA, Vialet-Chabrand S, Lawson T. 2018. Acclimation to fluctuating light impacts the rapidity of response and diurnal rhythm of stomatal conductance. Plant Physiology **176**, 1939–1951.

Matthews JSA, Vialet-Chabrand SRM, Lawson T. 2017. Diurnal variation in gas exchange: the balance between carbon fixation and water loss. Plant Physiology **174**, 614–623.

McAusland L, Vialet-Chabrand S, Davey P, Baker NR, Brendel O, Lawson T. 2016. Effects of kinetics of light-induced stomatal responses on photosynthesis and water-use efficiency. New Phytologist **211**, 1209–1220.

McElwain JC, Yiotis C, Lawson T. 2016. Using modern plant trait relationships between observed and theoretical maximum stomatal conductance and vein density to examine patterns of plant macroevolution. New Phytologist **209**, 94–103.

Messinger SM, Buckley TN, Mott KA. 2006. Evidence for involvement of photosynthetic processes in the stomatal response to CO_2. Plant Physiology **140**, 771–778.

Mott KA. 1988. Do stomata respond to CO_2 concentrations other than intercellular? Plant Physiology **86**, 200–203.

Mott KA, Gibson AC, O'Leary JW. 1982. The adaptive significance of amphistomatic leaves. Plant, Cell & Environment **5**, 455–460.

Mott KA, O'Leary JW. 1984. Stomatal behavior and CO_2 exchange characterisitcs in amphistomatous leaves. Plant Physiology **74**, 47–51.

Nunes TD, Slawinska MW, Lindner H, Raissig MT. 2022. Quantitative effects of environmental variation on stomatal anatomy and gas exchange in a grass model. Quantitative Plant Biology **3**, e6.

Ort DR, Long SP. 2014. Limits on yields in the Corn Belt. Science **344**, 484–485.

Ozeki K, Miyazawa Y, Sugiura D. 2022. Rapid stomatal closure contributes to higher water use efficiency in major C_4 compared to C_3 Poaceae crops. Plant Physiology **189**, 188–203.

Pan L, George-Jaeggli B, Borrell A, Jordan D, Koller F, Al-Salman Y, Ghannoum O, Cano FJ. 2022. Coordination of stomata and vein patterns with leaf width underpins water-use efficiency in a C_4 crop. Plant, Cell & Environment **45**, 1612–1630.

Papanatsiou M, Petersen J, Henderson L, Wang Y, Christie JM, Blatt MR. 2019. Optogenetic manipulation of stomatal kinetics improves carbon assimilation, water use, and growth. Science **363**, 1456–1459.

Parsons R, Weyers JDB, Lawson T, Godber IM. 1998. Rapid and straightforward estimates of photosynthetic characteristics using a portable gas exchange system. Photosynthetica **34**, 265–279.

Pearcy RW. 1990. Sunflecks and photosynthesis in plant canopies. Annual Review of Plant Physiology and Plant Molecular Biology **41**, 421–453.

Pearcy RW, Ehleringer J. 1984. Comparative ecophysiology of C_3 and C_4 plants. Plant, Cell & Environment **7**, 1–13.

Pearcy RW, Way DA. 2012. Two decades of sunfleck research: looking back to move forward. Tree Physiology **32**, 1059–1061.

Pingali PL. 2012. Green revolution: impacts, limits, and the path ahead. Proceedings of the National Academy of Sciences, USA **109**, 12302–12308.

Qu M, Essemine J, Xu J, *et al*. 2020. Alterations in stomatal response to fluctuating light increase biomass and yield of rice under drought conditions. The Plant Journal **104**, 1334–1347.

Qu M, Hamdani S, Li W, *et al*. 2016. Rapid stomatal response to fluctuating light: an under-explored mechanism to improve drought tolerance in rice. Functional Plant Biology **43**, 727–738.

Raissig MT, Matos JL, Anleu Gil MX, *et al*. 2017. Mobile MUTE specifies subsidiary cells to build physiologically improved grass stomata. Science **355**, 1215–1218.

Rao PP, Birthal PS, Reddy BV, Rai KN, Ramesh S. 2006. Diagnostics of sorghum and pearl millet grains-based nutrition in India. International Sorghum and Millets Newsletter **47**, 93–96.

Raschke K. 1975. Stomatal action. Annual Review of Plant Physiology **26**, 309–340.

Ray DK, Mueller ND, West PC, Foley JA. 2013. Yield trends are insufficient to double global crop production by. PLoS One **8**, e66428.

R StudioTeam. 2020. RStudio: integrated development for R. Boston, MA: RStudio, PBC.

Santos MG, Davey PA, Hofmann TA, Borland A, Hartwell J, Lawson T. 2021. Stomatal responses to light, CO_2, and mesophyll tissue in *Vicia faba* and *Kalanchoë fedtschenkoi*. Frontiers in Plant Science **12**, 740534.

Schneider CA, Rasband WS, Eliceiri KW. 2012. NIH Image to ImageJ: 25 years of image analysis. Nature Methods **9**, 671–675.

Sharkey TD, Raschke K. 1981. Effect of light quality on stomatal opening in leaves of *Xanthium strumarium* L. Plant Physiology **68**, 1170–1174.

Spinoni J, Vogt JV, Naumann G, Barbosa P, Dosio A. 2018. Will drought events become more frequent and severe in Europe? International Journal of Climatology **38**, 1718–1736.

Stevens J, Jones MA, Lawson T. 2021. Diverse physiological and physical responses among wild, landrace and elite barley varieties point to novel breeding opportunities. Agronomy **11**, 921.

Taylor SH, Franks PJ, Hulme SP, Spriggs E, Christin PA, Edwards EJ, Woodward FI, Osborne CP. 2012. Photosynthetic pathway and ecological adaptation explain stomatal trait diversity amongst grasses. New Phytologist **193**, 387–396.

Ticha I. 1982. Photosynthetic characteristics during ontogenesis of leaves. 7. Stomata density and sizes. Photosynthetica **16**, 471.

USDA. 2022. Grain: world markets and trade. Washington, DC: United States Department of Agriculture.

Vialet-Chabrand S, Hills A, Wang Y, Griffiths H, Lew VL, Lawson T, Blatt MR, Rogers S. 2017a. Global sensitivity analysis of OnGuard models identifies key hubs for transport interaction in stomatal dynamics. Plant Physiology **174**, 680–688.

Vialet-Chabrand S, Matthews JS, Simkin AJ, Raines CA, Lawson T. 2017b. Importance of fluctuations in light on plant photosynthetic acclimation. Plant Physiology **173**, 2163–2179.

Vialet-Chabrand S, Matthews JSA, Lawson T. 2021. Light, power, action! Interaction of respiratory energy- and blue light-induced stomatal movements. New Phytologist **231**, 2231–2246.

Vialet-Chabrand SRM, Matthews JSA, McAusland L, Blatt MR, Griffiths H, Lawson T. 2017c. Temporal dynamics of stomatal behavior: modeling and implications for photosynthesis and water use. Plant Physiology **174**, 603–613.

Vico G, Manzoni S, Palmroth S, Katul G. 2011. Effects of stomatal delays on the economics of leaf gas exchange under intermittent light regimes. New Phytologist **192**, 640–652.

Wall S, Vialet-Chabrand S, Davey P, Van Rie J, Galle A, Cockram J, Lawson T. 2022. Stomata on the abaxial and adaxial leaf surfaces contribute differently to leaf gas exchange and photosynthesis in wheat. New Phytologist **235**, 1743–1756.

Way DA, Katul GG, Manzoni S, Vico G. 2014. Increasing water use efficiency along the C_3 to C_4 evolutionary pathway: a stomatal optimization perspective. Journal of Experimental Botany **65**, 3683–3693.

Weyers JDB, Johansen LG. 1985. Accurate estimation of stomatal aperture from silicone rubber impressions. New Phytologist **101**, 109–115.

Wong S, Cowan I, Farquhar G. 1979. Stomatal conductance correlates with photosynthetic capacity. Nature **282**, 424–426.

WWAP. 2015. The United Nations World Water Development Report. Paris: UNESCO.

Xiong D, Flexas J. 2020. From one side to two sides: the effects of stomatal distribution on photosynthesis. New Phytologist **228**, 1754–1766.

Yamori W, Kusumi K, Iba K, Terashima I. 2020. Increased stomatal conductance induces rapid changes to photosynthetic rate in response to naturally fluctuating light conditions in rice. Plant, Cell & Environment **43**, 1230–1240.

Zhang N, Berman SR, Joubert D, Vialet-Chabrand S, Marcelis LFM, Kaiser E. 2022. Variation of photosynthetic induction in major horticultural crops is mostly driven by differences in stomatal traits. Frontiers in Plant Science **13**, 860229.